Received: 23 November 2017 | Revised: 20 February 2018 | Accepted: 21 February 2018

DOI: 10.1111/cas.13557

ORIGINAL ARTICLE

WILEY Cancer Science

Droplet digital polymerase chain reaction assay and peptide nucleic acid-locked nucleic acid clamp method for *RHOA* mutation detection in angioimmunoblastic T-cell lymphoma

Sharna Tanzima Nuhat[1] | Mamiko Sakata-Yanagimoto[2] | Daisuke Komori[1] | Keiichiro Hattori[1] | Yasuhito Suehara[1] | Kota Fukumoto[1] | Manabu Fujisawa[1] | Manabu Kusakabe[2] | Kosei Matsue[3] | Hirotake Wakamatsu[4] | Mitsunobu Shimadzu[4] | Shigeru Chiba[2,5]

[1]Department of Hematology, Graduate School of Comprehensive Human Sciences, University of Tsukuba, Tsukuba, Japan

[2]Department of Hematology, Faculty of Medicine, University of Tsukuba, Tsukuba, Japan

[3]Division of Hematology/Oncology, Department of Internal Medicine, Kameda Medical Center, Kamogawa, Japan

[4]LSI Medience Co., Tokyo, Japan

[5]Life Science Centre of Tsukuba Advanced Research Alliance University of Tsukuba, Tsukuba, Japan

Correspondence
Mamiko Sakata-Yanagimoto and Shigeru Chiba, Department of Hematology, Faculty of Medicine, University of Tsukuba, Tsukuba, Japan.
Emails: sakatama-tky@umin.net; schiba-tky@umin.net

Funding information
Ministry of Education, Culture, Sports, and Science of Japan (16H02660), Practical Research for Innovative Cancer Control from Japan Agency for Medical Research and Development, AMED, Kobayashi Foundation for Cancer Research, Leukemia Research Fund, and Takeda Science Foundation for Cancer Research.

Angioimmunoblastic T-cell lymphoma (AITL) is a subtype of nodal peripheral T-cell lymphoma (PTCL). Somatic *RHOA* mutations, most frequently found at the hotspot site c.50G > T, p.Gly17Val (G17V *RHOA* mutation) are a genetic hallmark of AITL. Detection of the G17V *RHOA* mutations assists prompt and appropriate diagnosis of AITL. However, an optimal detection method for the G17V *RHOA* mutation remains to be elucidated. We compared the sensitivity and concordance of next-generation sequencing (NGS), droplet digital PCR (ddPCR) and peptide nucleic acid-locked nucleic acid (PNA-LNA) clamp method for detecting the G17V *RHOA* mutation. G17V *RHOA* mutations were identified in 27 of 67 (40.3%) PTCL samples using NGS. ddPCR and PNA-LNA clamp method both detected G17V mutations in 4 samples in addition to those detected with NGS (31 of 67, 46.3%). Additionally, variant allele frequencies with ddPCR and those with NGS showed high concordance ($P < .001$). Three other *RHOA* mutations involving the p.Gly17 position (c.[49G > T;50G > T], p.Gly17Leu in PTCL198; c.[50G > T;51A > C], p.Gly17Val in PTCL216; and c.50G > A, p.Gly17Glu in PTCL223) were detected using NGS. These sequence changes could not appropriately be detected using the ddPCR assay and the PNA-LNA clamp method although both indicated that the samples might have mutations. In total, 34 out of 67 PTCL samples (50.7%) had *RHOA* mutations at the p.Gly17 position. In conclusion, our results suggested that a combination of ddPCR/PNA-LNA clamp methods and NGS are best method to assist the diagnosis of AITL by detecting *RHOA* mutations at the p.Gly17 position.

KEYWORDS
angioimmunoblastic T-cell lymphoma, droplet digital polymerase chain reaction (ddPCR) assay, G17V *RHOA* mutation, next-generation sequencing (NGS), PNA-LNA clamp method

1 | INTRODUCTION

ngioimmunoblastic T-cell lymphoma (AITL) is a distinct subtype of nodal peripheral T-cell lymphoma (PTCL).[1] A large percentage of patients (68%-94%) present with advanced-stage disease (stages III-IV) at diagnosis.[2] High fever, skin rash, hepatosplenomegaly, pleural effusions, and generalized lymphadenopathy are predominant clinical features of AITL. Autoimmune-like manifestations including hemolytic anemia and polyclonal hypergammaglobulinemia are also frequently observed. AITL tumor cells display features of follicular helper T (T_{FH}) cells.[3] Recurrent genetic abnormalities frequently found in AITL include mutations in *RHOA* (50%-70%),[4-6] *TET2* (47%-83%),[4,7,8] *IDH2* (20%-45-%),[4,9] *DNMT3A* (20%-30%),[4,7,10] and *CD28* (9.4%-11.3%).[11-13] The vast majority of *RHOA* mutations found in AITL are c.50G > T, p.Gly17Val (G17V *RHOA* mutations),[4-6] although different *RHOA* mutations at the p.Gly17 position (c.49_51del, p.Gly17del,[4] c.[50G > T;51A > C], p.Gly17Leu,[14] and c.50G > A, p.Gly17Leu[6]) were reported. Peripheral T-cell lymphoma, not otherwise specified (PTCL-NOS) is a T-cell lymphoma that cannot be categorized into any subtypes of PTCL (although some PTCL-NOS cases show tumor cells with T_{FH}-like features[4,8]).[1] In 2016, the revised WHO classification used an umbrella category for nodal T-cell lymphomas with T_{FH} phenotype that comprise AITL, follicular T-cell lymphoma (FTCL), and nodal PTCL with T_{FH} phenotype.[1] The G17V *RHOA* mutations, which are extremely rare in the other hematological cancers, are found in approximately 60% of cases of nodal PTCL with T_{FH} phenotype.[4,11] The frequent and specific distribution of G17V *RHOA* mutations in AITL and nodal PTCL with T_{FH} phenotype highlights the diagnostic value of this mutation for these subtypes of PTCL.

In clinical practice, routine detection of G17V *RHOA* mutations is challenging as a result of the low ratio of tumor cells in AITL tissues. Additionally, insufficient quality of genomic DNA derived from biopsy specimens hinders efficient and robust mutation testing. Hence, optimized methods capable of overcoming these problems are needed for detecting G17V *RHOA* mutations in the clinical setting. In the present study, we carried out extensive analyses of G17V *RHOA* mutations using droplet digital PCR (ddPCR), peptide nucleic acid-locked nucleic acid (PNA-LNA) clamp method, and next-generation sequencing (NGS) to clarify the concordance and sensitivity of these methods.

2 | MATERIALS AND METHODS

2.1 | Patients

Sixty-seven patients with PTCL (40 AITL and 27 PTCL-NOS) were included into this retrospective study (Table S1). The study was approved (approval numbers are H 24-74 and H 28-268) by the ethical committee of University of Tsukuba Hospital.

2.2 | Sample collection and DNA extraction

Genomic DNAs were extracted from frozen samples using a nucleospin tissue kit (Macherey-Nagel, Düren, Germany) according to the manufacturer's instructions. Concentrations of the extracted DNAs were measured using a Qubit 2.0 fluorometer (Thermo Fisher Scientific, Waltham, MA, USA). The extracted DNAs were stored at −20°C until use.

2.3 | Primer design and amplicon preparation for deep sequencing

Amplification reactions were carried out with 20 ng extracted genomic DNA as the template in a 10-μL reaction volume with Kod-Plus-Neo PCR reagent (TOYOBO, Osaka, Japan), and 300-nmol/L concentration of forward (5′-GCCCCATGGTTACCAAAGCA-3′) and reverse primers (5′-ACATGGAAAATGGCATCAGTTGTT-3′). The two-step cycling parameters used to amplify the PCR product were: 94°C for 2 minutes, 35 cycles at 98°C for 10 seconds, and at 68°C for 30 seconds. Amplicons were visualized on a 1% agarose gel stained with ethidium bromide.

2.4 | Library preparation and amplicon-based deep sequencing

Libraries were prepared from the PCR products using an IonPGM fragment library preparation kit (Thermo Fisher Scientific) as previously described.[15] Briefly, PCR amplicons were ligated to barcode adapters and P1 adapters before amplification. The amplified libraries were quantitated using quantitative PCR with the Ion Library Quantitation kit according to the manufacturer's instructions (Thermo Fisher Scientific). Libraries were then subjected to deep sequencing on the Ion Torrent PGM platform according to the standard protocol for 300 base-pair single-end reads (Thermo Fisher Scientific). Sequencing data were analyzed using Variant Caller 5.0 (Thermo Fisher Scientific). Results of *RHOA* mutation analysis of 50 PTCL samples using NGS were previously described (Table S2).[16]

2.5 | ddPCR assay

The PCR primer/probe mix for the G17V *RHOA* mutation was purchased from Bio-Rad (Hercules, CA, USA). The probe fluorophores used for mutant and wild-type DNA were FAM and HEX, respectively. A 20-μL reaction mixture containing 10 μL ddPCR supermix for probe (no dUTP) × 2 (Bio-Rad), 1 μL of 10 μmol/L primer/probe mix, and 40 ng DNA template was mixed with 70 μL droplet generation oil through microfluidics in the Droplet Generator (Bio-Rad). Following droplet generation, the water-in-oil droplets were transferred to a standard 96-well PCR plate, which was heat sealed with a foil plate seal (Bio-Rad) and placed on a Bio-Rad thermocycler for PCR amplification using the following protocol: 10 minutes at 95°C, followed by 40 cycles of 30 seconds at 94°C, and 60 seconds at 53.1°C, followed by a 10-minute hold at 98°C. Upon completion of the PCR, the plate was transferred to a Droplet Reader (Bio-Rad). The data were initially analyzed using QuantaSoft software (Bio-Rad). The fluorescence threshold was set at 5000 for FAM and 2000 for HEX. Wells with less than 3 positive oil droplets were considered as negative, except for wells with 2 positive droplets showing reproducible results, which were considered as positive.

2.6 | PNA-LNA PCR clamp method

For PNA-LNA PCR clamp, PCR primers (forward and reverse primers 200 nmol/L each), fluorogenic probes (total probe and LNA 100 nmol/L each), and a PNA clamp primer (50 nmol/L) were added to the Premix Ex taq (Probe qPCR) Master Mix (Takara, Shiga, Japan). Total probe (fluorescent dye Cy5) targeted normal sequences and LNA probe (fluorescent dye FAM) targeted the sequences with the G17V mutation. The primer and probe sequences used to detect the G17V *RHOA* mutations are listed in Table S3. Quantitative PCR was then carried out with a 30 seconds hold at 95°C followed by 45 cycles at 95°C for 3 seconds, and 62°C for 30 seconds.

2.7 | Statistical analysis

Statistical analysis was conducted using SPSS software (IBM Japan, Tokyo, Japan). The correlation between variant allele frequencies (VAF) from ddPCR assay and those from NGS was analyzed using Spearman's correlation coefficient. *P*-value <.05 was considered statistically significant.

3 | RESULTS

3.1 | Mutation detection sensitivity of ddPCR assay

At first, we established the lower limits of detection (LOD) and quantification (LOQ) for ddPCR assay. For this, serial dilution samples were prepared to make the VAF of the G17V mutation at 13%, 3.25%, 0.81%, 0.20%, 0.05%, 0.01%, and 0.0025%. WT genomic DNA and distilled water (DW) were used as negative control and no template control, respectively (Figure S1A). Analysis of the result using ddPCR assay showed highly concordant VAFs with input DNA templates (R^2 = .9996) (Figure S1A).

After being converted to log-log scale, data showed precision and linearity down to a dilution of 0.05%; which corresponded to a fractional abundance (proportion of the mutated DNA; QuantaSoft) of 0.06% (coefficient of determination [R^2] was .9996). The positive control diluted to 0.01% was also judged as positive using ddPCR assay, whereas the fractional abundance was 0.02% (Figure S1A). Mutant alleles at a frequency of <0.01% could not be detected and, thus, <0.01% was considered as negative.

For these reasons, LOQ of ddPCR assay was defined as 0.05% with a fractional abundance of 0.06%. Further experiments showed that LOD could be lowered to 0.01% with a fractional abundance of 0.02%.

3.2 | Mutation detection sensitivity of the PNA-LNA clamp method

Next, we investigated the detection limit of the PNA-LNA PCR clamp method for the G17V *RHOA* mutation. The mutant DNA was mixed with WT DNA to generate different dilution samples at 1%, 0.1%, 0.01%, and 0.001% (Figure S1B). The PNA-LNA PCR clamp method was able to detect the G17V *RHOA* sequence at dilutions down to 0.01% but not 0.001% (Figure S1B). Because of the limitation of this method, we could not measure the quantity of the mutations.

3.3 | Comparison of mutations detected by different methods

Using the data from the 67 PTCL samples we compared the concordance rates of the above-mentioned 3 methods (Table S2; Figure 1). c.50G > T, p.Gly17Val *RHOA* mutations were detected in 27 of the 67 PTCL samples (40.3%) (AITL 20/40 [50.0%], PTCL-NOS 7/27 [25.9%]) with NGS (Figure 1A,C; Table S2). ddPCR assay and PNA-LNA clamp method could detect low mutant alleles in 4 cases, which were not detected with NGS (PTCL171, PTCL186, PTCL209, and PTCL259; Figure 2). The mutation ratio according to ddPCR assay was 0.13%, 0.03%, 0.05%, and 0.21% for PTCL171, PTCL186, PTCL209, and PTCL259, respectively. Amplification curves of these samples produced using the PNA-LNA clamp method were also clearly distinguishable from the WT (Figure 2B). In total, 31 of 67 samples (46.3%) (AITL 23/40 [57.5%], PTCL-NOS 8/27 [29.6%]) were positive for the c.50G > T, p.Gly17Val *RHOA* mutations with both the ddPCR assay and the PNA-LNA method (Figure 1A,C; Table S2), indicating that the results of these two methods were 100% concordant for detecting positive and negative samples (Figure 1A,C; Table S2). Furthermore, the data showed that the ddPCR assay and the PNA-LNA method have higher sensitivity than NGS for detecting G17V *RHOA* mutations in samples.

According to the quantitative results of the ddPCR assay, mutation ratio in the ddPCR assay and VAF in NGS were statistically correlated (Spearman's correlation coefficient 0.868, *P*-value <.001) (Figure 3). Inter-method discrepancies more than double were found in 2 samples (PTCL252 with a VAF of 19.8% in NGS and a mutation ratio of 4.6% in ddPCR assay; PTCL245 with a VAF of 76.4% in NGS and a mutation ratio of 14.28% in ddPCR assay).

3.4 | Analysis of the other *RHOA* mutations at the p.Gly17 position using the ddPCR assay and the PNA-LNA clamp method

Three other *RHOA* mutations at the p.Gly17 position were detected using NGS: c.[49G > T;50G > T], p.Gly17Leu in PTCL198; c.[50G > T;51A > C], p.Gly17Val in PTCL216; and c.50G > A, p.Gly17Glu in PTCL223 instead of the c.50G > T, p.Gly17Val *RHOA* mutations (Fujisawa et al.[16] and Figure 4). As described above, we observed that the fluorescence amplitude of FAM-positive droplets in a reaction was more than 5000 for all c.50G > T mutation-positive samples with the ddPCR assay. However, those samples having the other *RHOA* mutations at the p.Gly17 position (PTCL198, PTCL216, and PTCL223) showed clusters of droplets lower than 5000, which were clearly separable from the WT droplets (Figure 4A). Furthermore, analysis of each of these samples using the PNA-LNA clamp method showed different crossing point (Cp) values

(A)

RHOA c.50G>T, p.Gly17Val mutation	ddPCR & PNA-LNA clamp			NGS			Either ddPCR, PNA-LNA clamp or NGS		
	AITL, *n* (%)	PTCLNOS, *n* (%)	Total, *n* (%)	AITL, *n* (%)	PTCLNOS, *n* (%)	Total, *n* (%)	AITL, *n* (%)	PTCLNOS, *n* (%)	Total, *n* (%)
Positive	23 (57.50%)	8 (29.63%)	31 (46.27%)	20 (50.00%)	7 (25.93%)	27 (40.30%)	23 (57.50%)	8 (29.63%)	31 (46.27%)
Negative	17 (42.50%)	19 (70.37%)	36 (53.73%)	20 (50.00%)	20 (74.07%)	40 (59.70%)	17 (42.50%)	19 (70.37%)	36 (53.73%)

(B)

RHOA mutation	ddPCR & PNA-LNA clamp			NGS			Either ddPCR, PNA-LNA clamp or NGS		
	AITL, *n* (%)	PTCLNOS, *n* (%)	Total, *n* (%)	AITL, *n* (%)	PTCLNOS, *n* (%)	Total, *n* (%)	AITL, *n* (%)	PTCLNOS, *n* (%)	Total, *n* (%)
Positive	23 (57.50%)	8 (29.63%)	31 (46.27%)	23 (57.50%)	7 (25.93%)	30 (44.78%)	26 (65.00%)	8 (29.63%)	34 (50.74%)
Negative	17 (42.50%)	19 (70.37)	36 (53.73%)	17 (42.50%)	20 (74.07%)	37 (55.22%)	14 (35.00%)	19 (70.37%)	33 (49.26%)

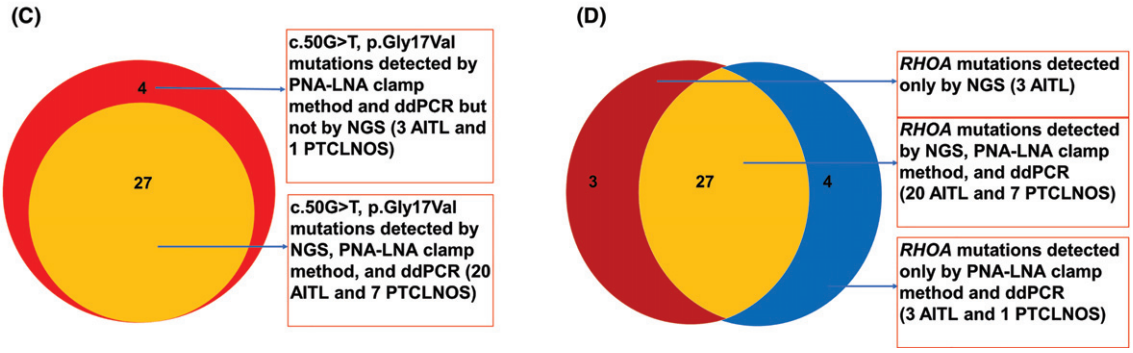

FIGURE 1 Study profile. A,B, Frequencies of A, *RHOA* c.50G > T, p.Gly17Val mutations, and B, total *RHOA* mutations detected by droplet digital PCR (ddPCR) assay and peptide nucleic acid-locked nucleic acid (PNA-LNA) method, and next generation sequencing (NGS); and either ddPCR assay, PNA-LNA clamp method or NGS. AITL, angioimmunoblastic T-cell lymphoma; PTCL-NOS, peripheral T-cell lymphoma, not otherwise specified. C,D, Venn diagrams of the frequencies of C, *RHOA* c.50G > T, p.Gly17Val mutations, and D, total *RHOA* mutations detected by ddPCR assay, PNA-LNA method and NGS

of the amplification curves from those of either WT or the G17V *RHOA* mutations (Figure 4C). Experiments using the c.50G > T, p.Gly17Val probe did not show amplification in these samples, similar to those without the p.Gly17 *RHOA* mutations (Figure 4C). Total probe detected amplification, which was not appropriately clamped by addition of PNA (Figure 4D). The cutoff Cp value of WT with total probe was > 34. The Cp values in PTCL198, PTCL216, and PTCL223 with total probe were 28.63, 27.09, and 31.18, respectively, indicating that they are <34 in PTCL samples.

Further experiments with Sanger sequencing confirmed other *RHOA* mutations (c.[49G > T;50G > T], p.Gly17Leu in PTCL198; and c.[50G > T;51A > C], p.Gly17Val in PTCL216; and c.50G > A, p.Gly17Glu in PTCL223, respectively) at the p.Gly17 position (Figure 4B) which were previously detected by NGS. These data indicate that the ddPCR assay and the PNA-LNA clamp method could predict mutations around the p.Gly17 position, although neither method could determine the exact mutation type.

In total, *RHOA* mutations at the p.Gly17 position were found in 34 out of 67 PTCL samples (50.7%) (AITL 26/40 [65.0%], PTCL-NOS 8/27 [29.6%]) by either NGS, ddPCR assay or the PNA-LNA clamp method (Table S2; Figure 1B,D). We found that the results of the ddPCR and PNA-LNA clamp methods were concordant ($\kappa = 1$ and $P < .0001$). In addition, the kappa and *P*-values were .82 and <.0001, respectively, for both ddPCR and NGS, and PNA-LNA clamp method and NGS. We considered those samples as true positive which were positive by at least 2 methods (among ddPCR, PNA-LNA clamp method, NGS, and Sanger sequencing). Moreover, those samples that were negative by all 4 above-mentioned methods were considered as true negative. There were no samples in which *RHOA* mutations were detected by 1 method only. As a result, the sensitivity of

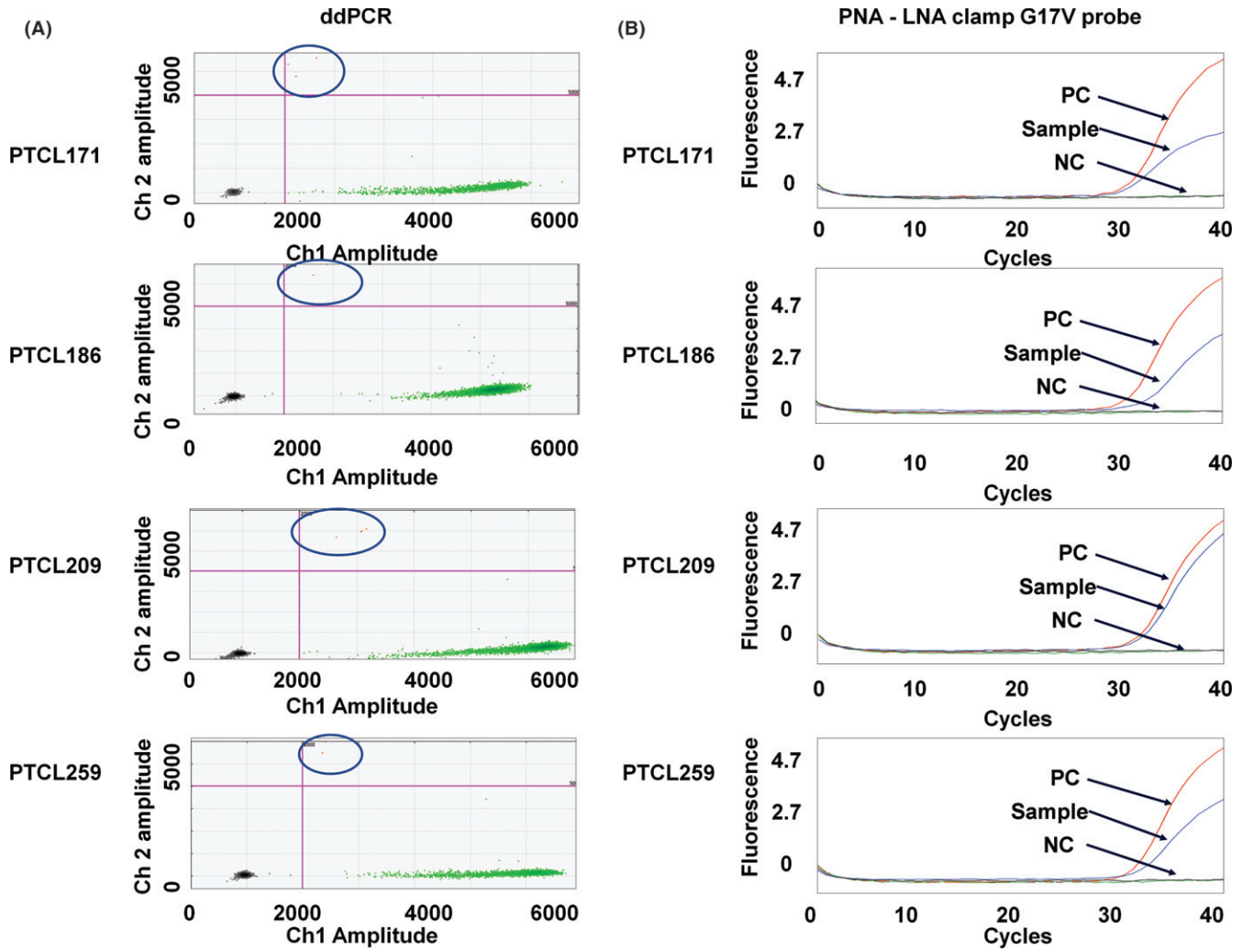

FIGURE 2 Detection of low-frequency mutations of G17V *RHOA* using droplet digital PCR (ddPCR) assay and peptide nucleic acid-locked nucleic acid (PNA-LNA) clamp method with G17V probe. A, 2D images of ddPCR analysis of samples PTCL171, PTCL186, PTCL209, and PTCL259. Pink color lines indicate FAM (horizontal) and HEX (vertical) threshold. B, Amplification curves produced by PNA-LNA clamp method with G17V probe for samples PTCL171, PTCL186, PTCL209, and PTCL259. PTCL, peripheral T-cell lymphoma. NC, negative control; PC, positive control

ddPCR and PNA-LNA clamp method for detection of c.50G > T, p.Gly17Val mutation was 100% (31/31) with 100% (36/36) specificity, whereas NGS had 87% (27/31) sensitivity with 100% (36/36) specificity. In contrast, for detection of all *RHOA* mutations at position 17, ddPCR and the PNA-LNA clamp method had 91% (31/34) sensitivity with 100% (33/33) specificity, and NGS had 88% (30/34) sensitivity with 100% (33/33) specificity.

4 | DISCUSSION

RHOA mutation detection has been increasingly focused for diagnosis of AITL and PTCL with T_{FH} phenotype.[14,17] Herein, we clarified that the ddPCR assay and the PNA-LNA clamp method could detect low allele mutations with extremely high sensitivity. In addition, mutation quantification by ddPCR assay showed results concordant with those by NGS. Although we found some discordances in VAF of 2 samples (PTCL245 and PTCL252), insufficient DNA quantity and quality may account for the discordant results, which is sometimes experienced in clinical settings. In contrast, the other *RHOA* mutations at the p.Gly17 position, which were detected by NGS could not be appropriately detected by either ddPCR assay or the PNA-LNA clamp method. As a result, combination of these methods increased the detection rate of *RHOA* mutations at the p.Gly17 position. We recently reported essential downstream signaling of G17V *RHOA* mutations in PTCL: the G17V mutant *RHOA* hyper-activated the T-cell receptor (TCR) signaling pathway through specific binding to VAV1 protein, an essential component in TCR signaling.[16] The other *RHOA* mutants at the p.Gly17 position presumably have a similar function, although it has not been examined.

There are several well-established methods to detect gene mutations in cancers. Among them, NGS has attracted attention over the past few years as a possible method for mutational analysis. Although the sensitivity of NGS is superior to that of direct

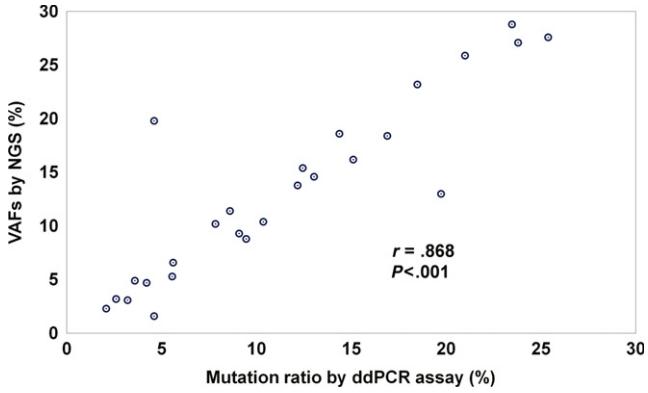

FIGURE 3 Comparison of mutational load quantified using droplet digital PCR (ddPCR) assay and next generation sequencing (NGS). Direct comparison of mutation ratio by ddPCR assay and variant allele frequencies (VAF) using NGS

sequencing, our findings suggest that NGS cannot detect low allele mutations.

Recently, the ddPCR assay has been widely used to detect genetic and epigenetic alterations.[18-21] ddPCR can detect very rare sequences with high precision and sensitivity by partitioning individual target molecules within distinct compartments and, therefore, reduces the limitations of conventional methods such as classic real-time quantitative PCR (qPCR) or the amplification refractory mutation system qPCR (ARMS qPCR).[22-24] However, the PNA-LNA clamp method is a molecular probe-based PCR method; its unique design and allele-specific approach allow exceptionally high specificity and sensitivity.[25,26] The NGS platform is more convenient for massive parallel sequencing of known and unknown mutations in multiple genes.[27] In contrast, to detect a known target mutation within a single gene, both the

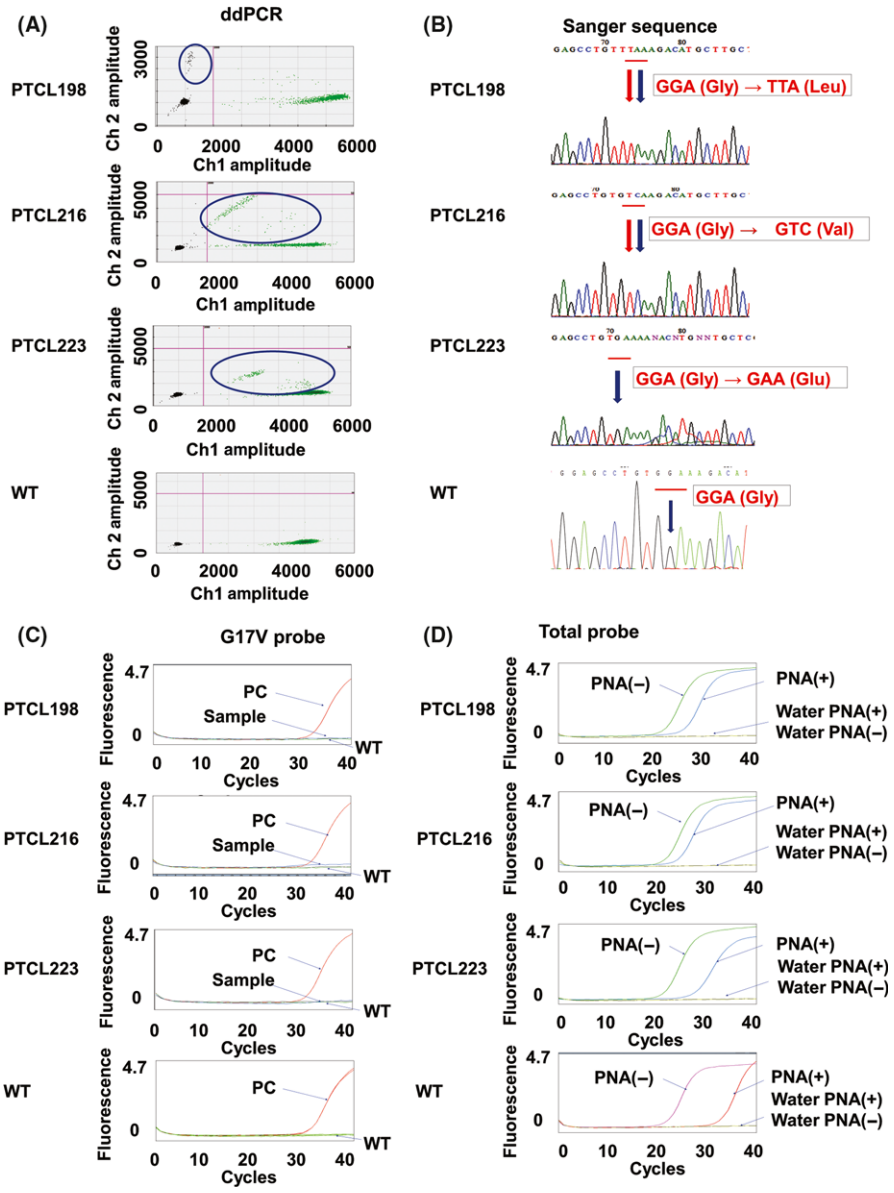

FIGURE 4 Samples having *RHOA* mutations at the p.Gly17 position other than c.50G > T, which could not be detected with droplet digital PCR (ddPCR) assay. A, 2D image of ddPCR assay of samples PTCL198, PTCL216, PTCL223, and wild type (WT). Pink color lines indicate FAM (horizontal) and HEX (vertical) threshold. B, Sanger sequencing result of samples PTCL198, PTCL216, PTCL223, and WT. C, Amplification curve produced by peptide nucleic acid-locked nucleic acid (PNA-LNA) clamp method with G17V probe for samples PTCL198, PTCL216, PTCL223, and WT. D, Amplification curve produced by PNA-LNA clamp method with total probe for samples PTCL198, PTCL216, PTCL223, and WT

ddPCR assay and the PNA-LNA clamp method have an economical advantage over NGS. The latter is not a quantitative method, because it relies on the threshold and quantification cycle (Cq) value for interpretation of the result, whereas ddPCR is independent of the Cq value and requires a relatively small amount of initial DNA.[23,24] However, the PNA-LNA clamp method is less expensive and clinically more accessible for mutation screening compared to ddPCR or NGS.[28]

To date, quantitative allele-specific PCR and other methods are being tried to detect the G17V *RHOA* mutation.[17] Several hotspot mutations such as V617F *JAK2* in myeloproliferative neoplasms,[29] V600E *BRAF* in hairy cell leukemia,[30] L265P *MYD88* in Waldenström macroglobulinemia,[31] and D661Y/Y640F/S614R *STAT3* in large granular lymphocytic leukemia[32] are being used for diagnostic purposes by means of NGS,[33] ddPCR,[34] ARMS-PCR,[35] allele-specific PCR,[36] high resolution melting,[37] qPCR,[38] and so on. The present study is the first report to evaluate the use of the ddPCR assay and the PNA-LNA clamp method for detection of low abundance *RHOA* G17V mutation.

In conclusion, our findings shed light on the potential of these techniques for the molecular diagnosis of AITL.

ACKNOWLEDGMENTS

This work was supported by Grants-in-Aid for Scientific Research (16H02660 to S.C.) from the Ministry of Education, Culture, Sports, and Science of Japan. This research was also partially supported by the Practical Research for Innovative Cancer Control from Japan Agency for Medical Research and Development, AMED, Kobayashi Foundation for Cancer Research, Leukemia Research Fund, and Takeda Science Foundation for Cancer Research to M.S.-Y.

CONFLICT OF INTEREST

Authors declare no conflicts of interest for this article.

ORCID

Sharna Tanzima Nuhat http://orcid.org/0000-0002-1516-9568
Keiichiro Hattori http://orcid.org/0000-0002-0810-7887
Kota Fukumoto http://orcid.org/0000-0002-2729-5780
Manabu Kusakabe http://orcid.org/0000-0003-2518-0776
Kosei Matsue http://orcid.org/0000-0002-8669-9865

REFERENCES

1. Swerdlow SH, Campo E, Pileri SA, et al. The 2016 revision of the World Health Organization classification of lymphoid neoplasms. *Blood*. 2016;127:2375-2390.
2. de Leval L, Gisselbrecht C, Gaulard P. Advances in the understanding and management of angioimmunoblastic T-cell lymphoma. *Br J Haematol*. 2010;148:673-689.
3. de Leval L, Rickman DS, Thielen C, et al. The gene expression profile of nodal peripheral T-cell lymphoma demonstrates a molecular link between angioimmunoblastic T-cell lymphoma (AITL) and follicular helper T (TFH) cells. *Blood*. 2007;109:4952-4963.
4. Sakata-Yanagimoto M, Enami T, Yoshida K, et al. Somatic RHOA mutation in angioimmunoblastic T cell lymphoma. *Nat Genet*. 2014;46:171-175.
5. Yoo HY, Sung MK, Lee SH, et al. A recurrent inactivating mutation in RHOA GTPase in angioimmunoblastic T cell lymphoma. *Nat Genet*. 2014;46:371-375.
6. Palomero T, Couronne L, Khiabanian H, et al. Recurrent mutations in epigenetic regulators, RHOA and FYN kinase in peripheral T cell lymphomas. *Nat Genet*. 2014;46:166-170.
7. Couronne L, Bastard C, Bernard OA. TET2 and DNMT3A mutations in human T-cell lymphoma. *N Engl J Med*. 2012;366:95-96.
8. Lemonnier F, Couronne L, Parrens M, et al. Recurrent TET2 mutations in peripheral T-cell lymphomas correlate with TFH-like features and adverse clinical parameters. *Blood*. 2012;120:1466-1469.
9. Cairns RA, Iqbal J, Lemonnier F, et al. IDH2 mutations are frequent in angioimmunoblastic T-cell lymphoma. *Blood*. 2012;119:1901-1903.
10. Dobay MP, Lemonnier F, Missiaglia E, et al. Integrative clinicopathological and molecular analyses of angioimmunoblastic T-cell lymphoma and other nodal lymphomas of follicular helper T-cell origin. *Haematologica*. 2017;102:e148-e151.
11. Vallois D, Dobay MP, Morin RD, et al. Activating mutations in genes related to TCR signaling in angioimmunoblastic and other follicular helper T-cell-derived lymphomas. *Blood*. 2016;128:1490-1502.
12. Rohr J, Guo S, Huo J, et al. Recurrent activating mutations of CD28 in peripheral T-cell lymphomas. *Leukemia*. 2016;30:1062-1070.
13. Lee SH, Kim JS, Kim J, et al. A highly recurrent novel missense mutation in CD28 among angioimmunoblastic T-cell lymphoma patients. *Haematologica*. 2015;100:e505-e507.
14. Nagao R, Kikuti YY, Carreras J, et al. Clinicopathologic analysis of angioimmunoblastic T-cell lymphoma with or without RHOA G17V mutation using formalin-fixed paraffin-embedded sections. *Am J Surg Pathol*. 2016;40:1041-1050.
15. Nguyen TB, Sakata-Yanagimoto M, Nakamoto-Matsubara R, et al. Double somatic mosaic mutations in TET2 and DNMT3A–origin of peripheral T cell lymphoma in a case. *Ann Hematol*. 2015;94:1221-1223.
16. Fujisawa M, Sakata-Yanagimoto M, Nishizawa S, et al. Activation of RHOA-VAV1 signaling in angioimmunoblastic T-cell lymphoma. *Leukemia*. 2017;32:694-702.
17. Nakamoto-Matsubara R, Sakata-Yanagimoto M, Enami T, et al. Detection of the G17V RHOA mutation in angioimmunoblastic T-cell lymphoma and related lymphomas using quantitative allele-specific PCR. *PLoS One*. 2014;9:e109714.
18. Preobrazhenskaya EV, Bizin IV, Kuligina ES, et al. Detection of BRCA1 gross rearrangements by droplet digital PCR. *Breast Cancer Res Treat*. 2017;165:765-770.
19. van Ginkel JH, Huibers MMH, van Es RJJ, de Bree R, Willems SM. Droplet digital PCR for detection and quantification of circulating tumor DNA in plasma of head and neck cancer patients. *BMC Cancer*. 2017;17:428.
20. Ye W, Tang X, Liu C, Wen C, Li W, Lyu J. Accurate quantitation of circulating cell-free mitochondrial DNA in plasma by droplet digital PCR. *Anal Bioanal Chem*. 2017;409:2727-2735.
21. Alcaide M, Yu S, Bushell K, et al. Multiplex droplet digital PCR quantification of recurrent somatic mutations in diffuse large B-Cell and follicular lymphoma. *Clin Chem*. 2016;62:1238-1247.
22. Sanders R, Huggett JF, Bushell CA, Cowen S, Scott DJ, Foy CA. Evaluation of digital PCR for absolute DNA quantification. *Anal Chem*. 2011;83:6474-6484.
23. Wang W, Song Z, Zhang Y. A Comparison of ddPCR and ARMS for detecting EGFR T790M status in ctDNA from advanced NSCLC

patients with acquired EGFR-TKI resistance. *Cancer Med*. 2017;6:154-162.
24. Zhang BO, Xu CW, Shao Y, et al. Comparison of droplet digital PCR and conventional quantitative PCR for measuring EGFR gene mutation. *Exp Ther Med*. 2015;9:1383-1388.
25. Yoshida H, Kim YH, Ozasa H, et al. EGFR T790M detection in circulating tumor dna from non-small cell lung cancer patients using the PNA-LNA clamp method. *Anticancer Res*. 2017;37:2721-2725.
26. Nagai Y, Miyazawa H, Huqun, et al. Genetic heterogeneity of the epidermal growth factor receptor in non-small cell lung cancer cell lines revealed by a rapid and sensitive detection system, the peptide nucleic acid-locked nucleic acid PCR clamp. *Cancer Res*. 2005;65:7276-7282.
27. Serratì S, De Summa S, Pilato B, et al. Next-generation sequencing: advances and applications in cancer diagnosis. *Onco Targets Ther*. 2016;9:7355-7365.
28. Sutani A, Nagai Y, Udagawa K, et al. Gefitinib for non-small-cell lung cancer patients with epidermal growth factor receptor gene mutations screened by peptide nucleic acid-locked nucleic acid PCR clamp. *Br J Cancer*. 2006;95:1483-1489.
29. Campo E, Swerdlow SH, Harris NL, Pileri S, Stein H, Jaffe ES. The 2008 WHO classification of lymphoid neoplasms and beyond: evolving concepts and practical applications. *Blood*. 2011;117:5019-5032.
30. Tiacci E, Trifonov V, Schiavoni G, et al. BRAF mutations in hairy-cell leukemia. *N Engl J Med*. 2011;364:2305-2315.
31. Treon SP, Hunter ZR. A new era for Waldenstrom macroglobulinemia: MYD88 L265P. *Blood*. 2013;121:4434-4436.
32. Koskela HL, Eldfors S, Ellonen P, et al. Somatic STAT3 mutations in large granular lymphocytic leukemia. *N Engl J Med*. 2012;366:1905-1913.
33. Hoogstraat M, Hinrichs JW, Besselink NJ, et al. Simultaneous detection of clinically relevant mutations and amplifications for routine cancer pathology. *J Mol Diagn*. 2015;17:10-18.
34. Rajasekaran N, Oh MR, Kim SS, et al. Employing digital droplet PCR to detect BRAF V600E mutations in formalin-fixed paraffin-embedded reference standard cell lines. *J Vis Exp*. 2015;53190. https://doi.org/10.3791/53190.
35. Jerez A, Clemente MJ, Makishima H, et al. STAT3 mutations unify the pathogenesis of chronic lymphoproliferative disorders of NK cells and T-cell large granular lymphocyte leukemia. *Blood*. 2012;120:3048-3057.
36. Xu L, Hunter ZR, Yang G, et al. Detection of MYD88 L265P in peripheral blood of patients with Waldenstrom's Macroglobulinemia and IgM monoclonal gammopathy of undetermined significance. *Leukemia*. 2014;28:1698-1704.
37. Thomas C, Amanuel B, Finlayson J, Grieu-Iacopetta F, Spagnolo DV, Erber WN. BRAF mutation detection in hairy cell leukaemia from archival haematolymphoid specimens. *Pathology*. 2015;47:349-354.
38. Chen P, Ouyang J, Liang J, Yu X, Huang B. Study on the clinical significance of JAK2V617F allele burden in philadelphia chromosome-negative myeloproliferative neoplasm. *Clin Lab*. 2016;62:1477-1481.

SUPPORTING INFORMATION

Additional Supporting Information may be found online in the supporting information tab for this article.

How to cite this article: Nuhat ST, Sakata-Yanagimoto M, Komori D, et al. Droplet digital polymerase chain reaction assay and peptide nucleic acid-locked nucleic acid clamp method for *RHOA* mutation detection in angioimmunoblastic T-cell lymphoma. *Cancer Sci*. 2018;109:1682-1689. https://doi.org/10.1111/cas.13557